ACS FOOD SCIENCE & TECHNOLOGY

Open Access

pubs.acs.org/acsfoodscitech

Article

ATR-FTIR Microspectroscopy as a Tool for Distinguishing Wine-Relevant *Saccharomyces* spp. Strains Based on Their Autolytic Behavior

Renato L. Binati, Nicola Ferremi Leali, Elisa Salvetti, Francesca Monti,* and Sandra Torriani

Cite This: *ACS Food Sci. Technol.* 2025, 5, 1625−1631

Read Online

ACCESS | Metrics & More | Article Recommendations

ABSTRACT: Yeast autolysis significantly impacts the final composition and sensory profile of wine, particularly in wine styles where postfermentation contact with yeast lees is encouraged. The release of macromolecules from yeast cells during autolysis is influenced by both the winemaking conditions and the intrinsic properties of the yeast strain. In this study, FTIR microspectroscopy in ATR mode coupled with multivariate statistical analysis was employed to monitor the autolytic process in YPD medium by analyzing the biochemical changes in the external cell structures of selected wine-relevant yeast strains: *Saccharomyces cerevisiae* EC 1118, FR-B, and CH, and *Saccharomyces bayanus* Q20. FTIR microspectroscopy allowed differentiating EC 1118 and FR-B from CH and Q20 based on the kinetics of the autolytic process mainly involving mannans and β-1,4 and β-1,6 glucans. As such, it has the potential for integration into the fine-tuned screening of starter cultures for biotechnological applications.

KEYWORDS: *FTIR microspectroscopy, starter cultures, Saccharomyces cerevisiae, Saccharomyces bayanus, autolysis, wine quality*

1. INTRODUCTION

Autolysis is an irreversible phenomenon occurring in yeast cells, associated with cell death at the end of the stationary phase of growth. Several intracellular enzymes are activated to carry out a cascade of reactions to degrade internal and external cell structures with subsequent release of the hydrolysis products into the surrounding medium. Although the autolytic process occurs naturally, in many industrial contexts it can be induced to achieve a faster conclusion of the degradation reactions leading to the production of yeast extracts. In the wine industry, natural autolysis is especially important for the production of wines with prolonged aging on dead yeast lees (e.g., Champagne, Muscadet), notably sparkling wines, but yeast autolysates obtained from induced autolysis are added to different wine styles to achieve flavor enhancements.[1,2]

Appealing yeast cell wall components for winemaking include proteins, peptides, and polysaccharides. The external structure of yeast cells is made of a network of mannoproteins, β-glucans, and chitin. Glucanases and proteases are the main autolytic enzymes involved in cell wall hydrolysis: glucanases hydrolyze the bonded glucans and mannoproteins, which are degraded later onto the protein and polysaccharide fractions by proteolysis. Subsequently, the breakdown of these components and the increased porosity of the cell wall facilitate the release of other cellular compounds, including lipids from plasma membrane degradation, as well as amino acids and ribonucleotides.[1,3,4]

Fourier-transform infrared (FTIR) microspectroscopy offers a reliable method for evaluating the autolysis capacity of new or established yeast starters.[5] This nondestructive technique allows for the collection of strain-specific absorbance spectra of microbial samples, requiring neither reagents nor extensive sample preparation. Band positions and intensities are interpreted as related to known biochemical functional groups and molecular bonds—such as those of proteins, lipids, carbohydrates, and nucleic acids—providing both qualitative and quantitative insights into the chemical composition of the samples.[6,7]

The analysis of yeast autolytic behavior in a defined growth medium, such as YPD (yeast, dextrose, peptone), using FTIR spectroscopy serves as an excellent screening tool for selecting strains for further in-depth evaluation in wine or wine model systems.[8] Moreover, it enables precise detection of oenologically significant molecules, such as mannans and glucans, facilitating their potential purification for various applications.[9]

In oenological research, FTIR spectroscopy has been more commonly applied for the inter- and intraspecific discrimination of yeasts from *Saccharomyces* and non-*Saccharomyces* species.[10−13] In one of the first studies,[14] FTIR spectroscopy has been successfully utilized to discriminate strains belonging to *Saccharomyces cerevisiae*, the most important wine yeast, and the closely related *Saccharomyces bayanus*. Other investigations targeted cell modifications and growth-dependent phenomena, including biochemical stress responses to dehydration[15,16] and biofilm-forming capacity.[8] Previous studies have demonstrated

Received: January 13, 2025
Revised: March 1, 2025
Accepted: March 10, 2025
Published: March 21, 2025

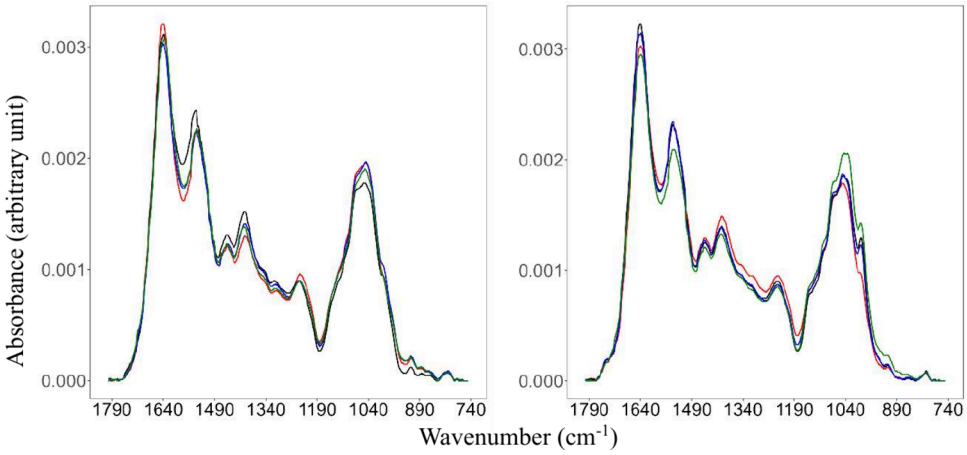

Figure 1. Area normalized average absorption spectra in the 1800−740 cm^{-1} range at day 0 (left) and day 5 (right) for *S. cerevisiae* EC 1118 (black), CH (red), FR-B (blue), and *S. bayanus* Q20 (green).

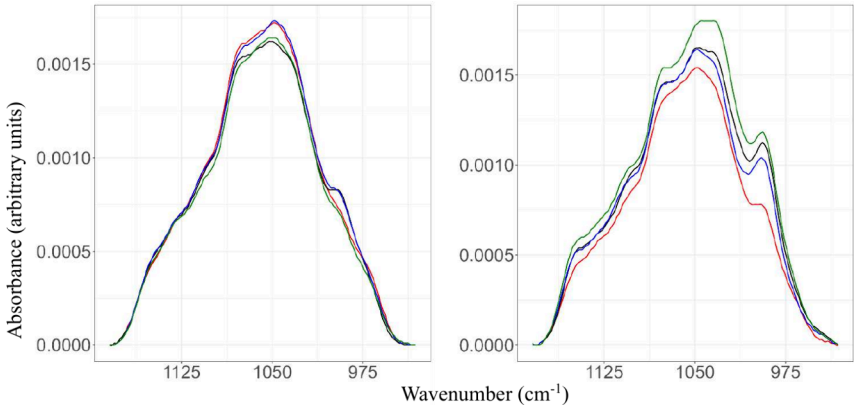

Figure 2. Area normalized average absorption spectra after baseline correction in the restricted range 1200−930 cm^{-1} at day 0 (left) and day 5 (right) for *S. cerevisiae* EC 1118 (black), CH (red), FR-B (blue), and *S. bayanus* Q20 (green).

that FTIR microspectroscopy is an effective tool for investigating the biochemical composition of yeast cells and analyzing structural changes associated with autolysis in *S. cerevisiae* EC 1118, a widely used industrial strain and a reference standard for sparkling wine production.[17,18] Recently,[19] FTIR spectroscopy was employed to compare the structure of yeast's mannans extracted through different methods, such as thermal hydrolysis and enzymatic hydrolysis, including autolysis.

The objective of this study was to apply mid-infrared FTIR microspectroscopy in conjunction with multivariate statistical analysis to investigate the cell wall biochemical composition of *Saccharomyces* spp. strains during incubation in a defined growth medium. The ultimate goal is to set up a procedure aimed at distinguishing between yeast strains, providing insight into their autolytic behavior; this will allow for the proper selection of the most promising strains to be used in biotechnological applications.

2. MATERIALS AND METHODS

2.1. Yeast Strains. The strains used in this study included *S. bayanus* Q20, a native strain isolated from Amarone wine, and three commercial strains of *S. cerevisiae*: CH (AEB spa, Brescia, Italy), EC 1118 (Lallemand Inc., Castel d'Azzano, Italy), and FR-B (Ferrari srl, Verona, Italy), which are well suited for producing white, sparkling, and red wines, respectively. CH and EC 1118 are also recognized as high mannoprotein and fine aroma producers. The *S. bayanus* Q20 strain produces low volatile acidity and high concentrations of secondary compounds. This strain is of interest both for its technological efficiency during alcoholic fermentation and for the quality of the resulting wines.[20] The pure cultures were isolated from dry active yeasts and used as wet cultures. All yeasts are cryopreserved at −80 °C in the yeast collection of the Department of Biotechnology, University of Verona (Verona University Culture Collection, Department of Biotechnology; VUCC-DBT).

2.2. Cultivation and Sampling. To monitor their autolytic capacity, samples of yeast cell cultures were collected at 0, 8, 24, 48, 96, and 120 h of incubation in YPD broth (10 g/L yeast extract, 20 g/L bacteriological peptone, 20 g/L dextrose; Sigma-Aldrich, Milan, Italy) under shaking (150 rpm) at 27 °C. Since it is known that the availability of nutrients, oxygen levels, temperature, pH, and other growth conditions influence the concentration of different parietal components,[21] all these conditions were standardized in this study to assess species- and strain-dependent characteristics. Unlike previous studies,[17,18] in the present investigation, autolysis was induced in a defined medium (YPD) as a screening method to distinguish between yeast strains and select the most promising ones.

The harvested samples (1 mL) of the investigated *Saccharomyces* spp. strains at six different time points were centrifuged (3000 × *g*, 10 min, 4 °C), and the obtained cell pellets were washed three times with saline solution (0.9% *w*/*v* NaCl).

2.3. FTIR Microspectroscopy. The cell pellets were resuspended in 500 μL of sterile water, and a 10 μL spot of each cellular suspension was deposited, in duplicate, on steel slides, which were previously washed with ultrapure water and ethanol 70% *v*/*v*. To dry the

https://doi.org/10.1021/acsfoodscitech.5c00022
ACS Food Sci. Technol. 2025, 5, 1625−1631

droplets, all slides were maintained under ventilation for 24 h, at 40 °C.

Mid-infrared absorption spectra were collected in the 1800−700 cm^{-1} range in the Attenuated Total Reflection (ATR) mode using a Vertex 70 Bruker Optics spectrometer coupled to a Hyperion 3000 vis/IR microscope (Bruker Optics, Germany). The system was equipped with a photoconductive MCT detector and a germanium ATR objective. The ATR mode has an enhanced sensitivity to the biochemical composition of the cell wall due to the reduced penetration depth of the infrared beam inside the sample, determined by the refractive indices of both the objective and the sample, that can be estimated to be around 400 nm at 1800 cm^{-1} up to 800 nm at 900 cm^{-1} in the present configuration. This depth, slightly increasing with the wavelength, is greater than the thickness of the cell wall but lower than the total thickness of the cell.[5] For each sample, i.e., for each time point, about 10 point-by-point spectra were acquired as the ratio of the transmitted to the incident photon intensity by coadding 256 scans at 4 cm^{-1} (108 s of acquisition time) from a 50 μm × 50 μm area.

2.4. Data Analysis. The software Opus 6.0 (Bruker Optics) was used for spectra pretreatment, including ATR and baseline correction, average spectra calculation, area normalization, and second derivative calculation to identify the main absorption bands. Principal Component Analysis (PCA) was performed using the statistical packages of the R software version 4.3.1.[22]

3. RESULTS AND DISCUSSION

To compare the biochemical characteristics of the studied *Saccharomyces* spp. strains at the beginning of incubation (day 0) and at the end of the autolytic process (day 5), the corresponding area normalized average absorption spectra are shown in Figure 1 in the 1800−740 cm^{-1} range. Since the most meaningful differences among the strains are observed in the 1200−930 cm^{-1} range, as expected from previous studies on different strains,[5] the absorption spectra before autolysis and after 5 days of autolysis after baseline correction in this restricted range are also shown, enlarged, in Figure 2.

Table 1 reports the most meaningful absorption bands, as identified through the second derivative on the average absorption spectra (Figure 3), and their corresponding assignments.

Table 1. Main Absorption Bands and Corresponding Assignments in the 1200−930 cm^{-1} Spectral Region for the ATR-FTIR Spectra of *Saccharomyces* spp.[5,18]

Absorption band (cm^{-1})	Main assignment
1150	C−O, C−OH carbohydrates, various contributions/ chitins
1130	β-1-3 glucans
1105	β-1-3 glucans
1080	phosphate
1045/1050[a]	mannans
1025/1030[a]	β-1,4 glucans
995/998[a]	β-1,6 glucans
968	mannans

[a]Absorption bands that were mostly affected by the autolytic process.

In ATR spectra, due to the limited infrared beam penetration depth inside the sample, the detected composition on each strain reflects the interplay between the relative concentrations of the various biochemical components within the entire cell and the relative thickness of the cell wall. Notably, in the 1200−930 cm^{-1} range, most relevant biochemical components[5] are primarily associated with the cell wall, except for the phosphate band at 1080 cm^{-1}, which is mainly related to intracellular nucleic acids and membrane phospholipids.

The behavior of second derivative spectra (Figure 3) at day 0 and after autolysis at day 5 highlights that the absorption bands that better discriminate the four spectra are those at 1050 cm^{-1} (mannans), 1030 cm^{-1} (β-1-4 glucans) and 995 cm^{-1} (β-1-6 glucans).

At day 0, the contribution of the band at 1050 cm^{-1} is either higher than or approximately equal to the band at 1030 cm^{-1} in CH and FR-B, respectively, whereas the opposite behavior is observed in EC 1118 and Q20, where the contribution of the 1030 cm^{-1} band is higher than that at 1050 cm^{-1}. Conversely, the band at 995 cm^{-1} is more intense in EC 1118 and FR-B, while it is lower in CH and Q20. The band at 1080 cm^{-1} exhibits a similar intensity across all strains.

After 5 days, the behavior of the 1080 cm^{-1} band differs among the four strains. The 1050 cm^{-1} band has the same intensity in all of the strains, while the 1030 cm^{-1} band increases and tends to be more intense than the 1050 cm^{-1} band, with the lowest intensity again observed in CH as compared to the other strains. The 995 cm^{-1} band increases in intensity in all of the strains relative to day 0, but it remains notably lower in CH as compared to the other strains.

To better highlight the effect of autolysis on each strain, absorption spectra at day 0 and at day 5 are compared strain by strain in Figure 4.

CH exhibits a distinct behavior, characterized by the lowest elevation in the 995 cm^{-1} band (β-1,6 glucans) as compared to all the other samples, while Q20 shows the most pronounced increase in the intensity of the 995 cm^{-1} band from days 0 to day 5. Both CH and FR-B show a relative decrease of 1050 cm^{-1} (mannans) and 1030 cm^{-1} (β-1,4 glucans) bands, while EC 1118 and Q20 exhibit a relative increase in the intensity of these bands, with a more prominent elevation in Q20.

To follow and compare the time evolution of the autolytic process in the four strains, PCA was applied to the average spectra at six time points (0, 8, 14, 48, 86, and 120 h) in the 1200−930 cm^{-1} range (Figure 4) on every single strain (Figure 5). In fact, PCA allows modeling the biological autolysis process, suggesting clustering of the samples as related to the autolysis kinetics.

The score plots display projections of the first two principal components, PC1 and PC2, of each spectrum at its corresponding time point, and the loading plots show the contributions of the various absorption bands to PC1 and PC2. PC1 captures the maximum variance within the data set, while PC2, orthogonal to PC1, accounts for the next largest variance, and so on for subsequent components. Interpreting the score plots with reference to the loading plots enables the identification of the absorption bands that mostly contribute to differentiation among the spectra, highlighting the time points at which the most meaningful changes occur.

As expected (Figure 5), the autolytic process mainly involves the 1050 cm^{-1} (mannans), the 1030 cm^{-1} (β-1,4 glucans), and the 995 cm^{-1} (β-1,6 glucans) bands. In CH and in Q20 (both starting with a low intensity of the β-1,6 band) time transitions are detected in PC1 (around 95% of the captured variance), while in EC 1118 and FR-B (both starting with a relatively high intensity of the β-1,6 band) time transitions involve both PC1 (around 60% of the captured variance) and PC2 (around 35% of the captured variance).

https://doi.org/10.1021/acsfoodscitech.5c00022
ACS Food Sci. Technol. 2025, 5, 1625−1631

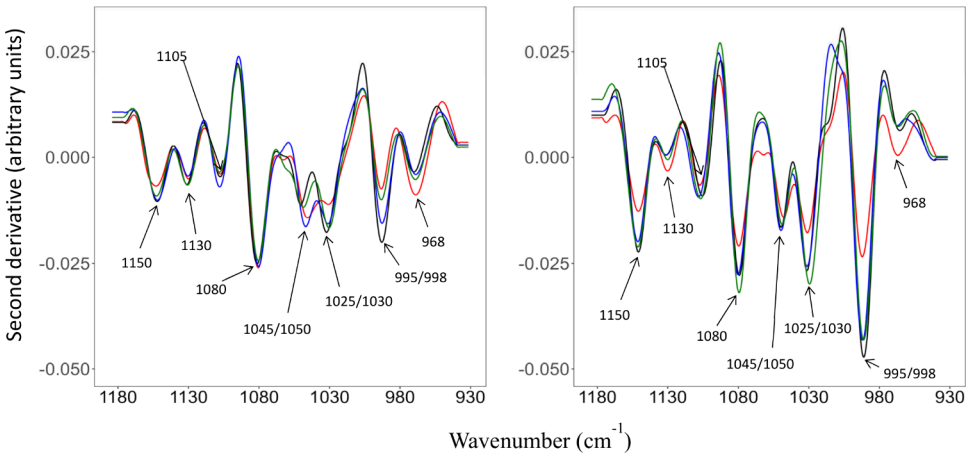

Figure 3. Second derivative plot of the FTIR spectra in the range 1200−930 cm^{-1} at 0 (left) and 120 h (right) for *S. cerevisiae* EC 1118 (black), CH (red), FR-B (blue), and *S. bayanus* Q20 (green).

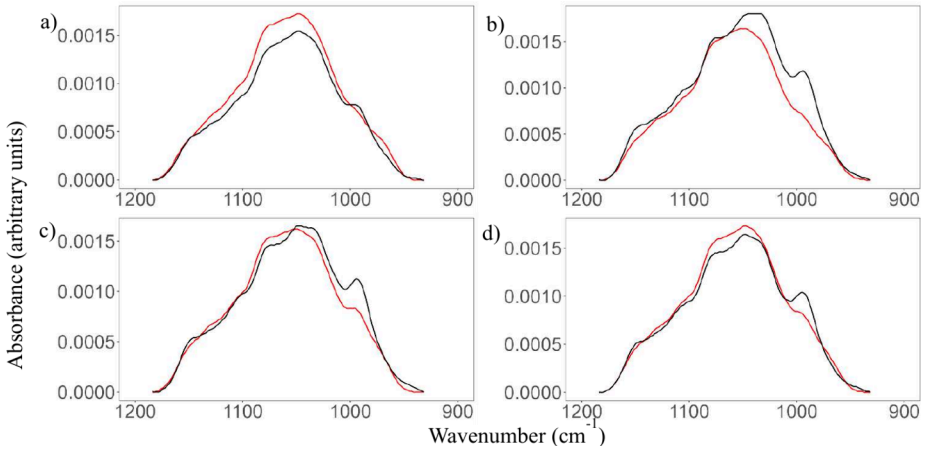

Figure 4. Area normalized average absorption spectra after baseline correction in the restricted range 1200−930 cm^{-1} at day 0 (red) and day 5 (black) for *S. cerevisiae* CH (a), *S. bayanus* Q20 (b), *S. cerevisiae* EC 1118 (c), and *S. cerevisiae* FR-B (d).

In CH (Figure 5a) a clear transition is visible in the PC1 from 24 to 48 h and is related to a relative increase of the 995 cm^{-1} band and a relative decrease of the 1050 and 1030 cm^{-1} bands (which were already higher than the 995 cm^{-1} at day 0, Figure 2). In Q20 (Figure 5b) two clear transitions are visible in PC1, the first one from 24 to 48 h and the second one from 48 to 96 h related to an increase of both 1050 cm^{-1} (together with 1030 cm^{-1}) and 995 cm^{-1} bands.

EC 1118 and FR-B (Figure 5c,d), which start at day 0 with a relatively higher 995 cm^{-1} band with respect to CH and Q20, show a similar temporal trend with a more gradual evolution, and PCA suggests the presence of two different processes with different timings.

In EC 1118, there is first an increase in both 1050 cm^{-1} (together with 1030 cm^{-1}) and 995 cm^{-1} bands between day 0 and 24 h (PC1), followed by a transition from 24 to 48 h where the 1050 and 1030 cm^{-1} bands decrease (PC1), while the 995 cm^{-1} one continues to increase up to 120 h (PC2). In FR-B there is first an increase in both 1050 cm^{-1} (together with 1030 cm^{-1}) and 995 cm^{-1} bands between day 0 and 48 h, followed by a transition from 48 to 96 h with a decrease in the 1050 cm^{-1} band.

These results suggest that in strains where the contribution of β-1,6 linkages is already high at day 0 (EC 1118 and FR-B), the autolytic process initially targets mannans and β-1,4 linkages, with β-1,6 degradation occurring at a later stage. In contrast, for strains with initially low levels of β-1,6 linkages (CH and Q20), the relative increase in β-1,6 linkages is already evident from the onset of the autolytic process.

To summarize, CH and Q20 showed greater stability, exhibiting a slower evolution throughout the autolysis process and inducing a less pronounced structural modification of the macromolecules, as compared to EC 1118 and FR-B. In contrast, EC 1118 and FR-B showed significantly faster reaction times, likely reflecting a higher release of cellular components into the medium. Previous studies have already demonstrated that EC 1118 progresses rapidly through the autolytic process in wine, particularly in the degradation of proteins and mannoproteins, with polysaccharide hydrolysis initiating at a later stage.[18]

PCA (Figure 5) highlights distinct differences between the strain pairs CH and Q20 vs EC1118 and FR-B. The CH and Q20 strains exhibit slower degradation of cellular endo-structures, initiating protease activity and accumulating hydrolysis products within the confines of the cell wall. Only after 24 h do the pores in the cell wall enlarge sufficiently to permit the release of these hydrolytic products into the surrounding medium.[1] In contrast, EC 1118 and FR-B display higher enzymatic activity within the first 24 h of incubation, as evidenced by a significant shift along PC1, driven by an

https://doi.org/10.1021/acsfoodscitech.5c00022
ACS Food Sci. Technol. 2025, 5, 1625−1631

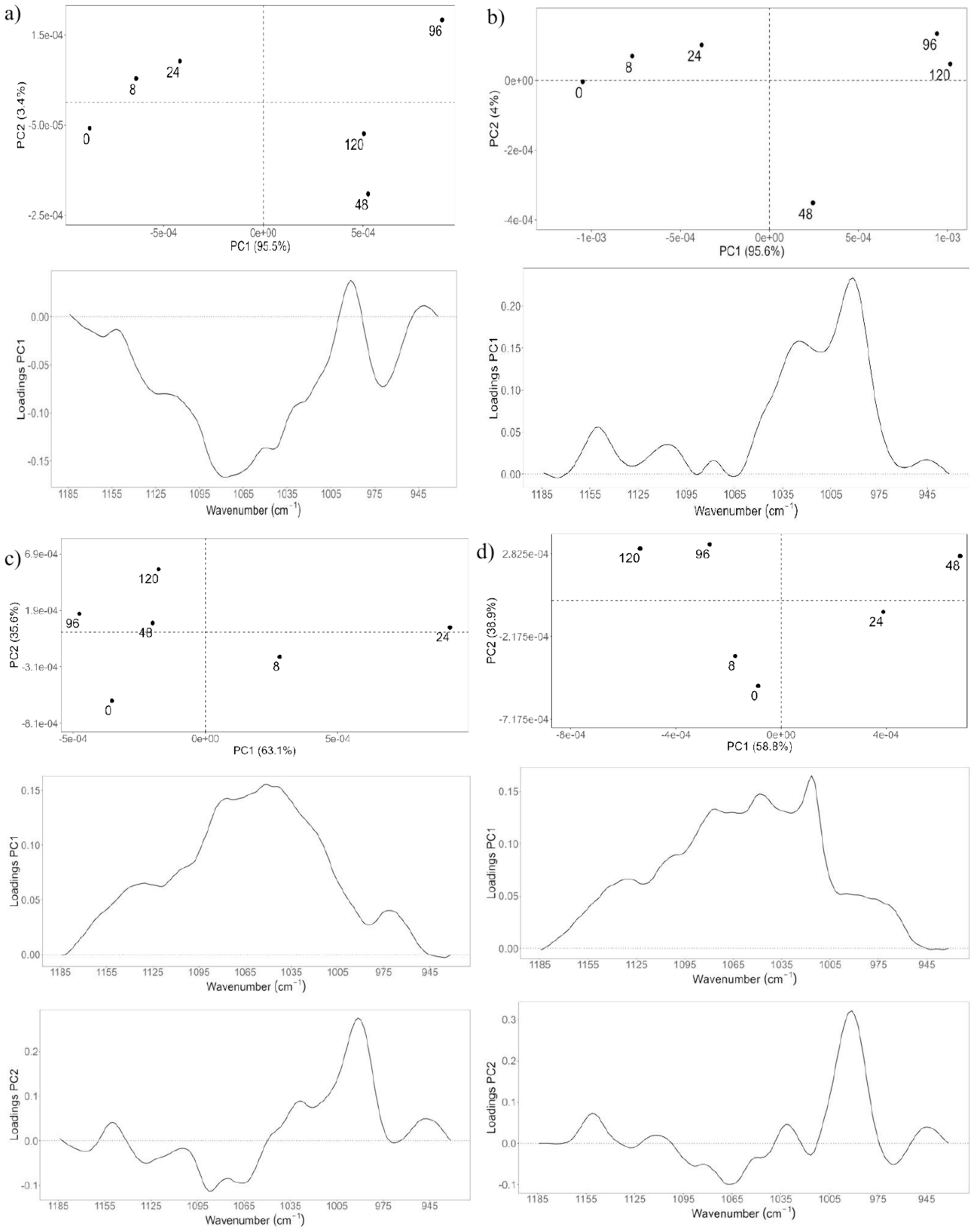

Figure 5. PCA score-plot and loadings of the average area normalized spectra in the 1200−930 cm^{-1} range for *S. cerevisiae* CH (a), *S. bayanus* Q20 (b), *S. cerevisiae* EC 1118 (c), *S. cerevisiae* FR-B (d) at 0, 8, 24, 48, 96, and 120 h.

increase in the 995 cm^{-1} band, which corresponds to the hydrolysis of cell wall β-glucans.

These results confirmed that the autolytic behavior and associated biochemical processes are strain-dependent, leading to the formation of two distinct strain clusters. In terms of temporal trends, CH and Q20 exhibited slower transitions, whereas EC 1118 showed the fastest evolution, followed by FR-B. Regarding biochemical modifications associated with cell

https://doi.org/10.1021/acsfoodscitech.5c00022
ACS Food Sci. Technol. 2025, 5, 1625−1631

lysis, EC 1118 displayed greater similarity to Q20, particularly in the degradation of β-1,6 glucans. Overall, this FTIR-based method proved to be an effective tool for distinguishing between yeast strains, enabling the screening of starters for wine styles in which yeast autolysis is a key factor in determining wine quality.

In the future, this valuable method could also be applied to evaluate the autolytic behavior of non-*Saccharomyces* yeast strains that are increasingly used in winemaking to differentiate the sensory profile of wine.

AUTHOR INFORMATION

Corresponding Author

Francesca Monti − *Department of Computer Science, University of Verona, 37134 Verona, Italy;* orcid.org/0000-0001-9488-7551; Email: francesca.monti@univr.it; Fax: +39 045 802 7910

Authors

Renato L. Binati − *Department of Biotechnology, University of Verona, 37134 Verona, Italy;* orcid.org/0000-0003-1979-5440

Nicola Ferremi Leali − *Department of Biotechnology, University of Verona, 37134 Verona, Italy;* orcid.org/0000-0001-8984-8486

Elisa Salvetti − *Department of Biotechnology, University of Verona, 37134 Verona, Italy; Verona University Culture Collection − Dept. of Biotechnology (VUCC-DBT), University of Verona, 37134 Verona, Italy*

Sandra Torriani − *Department of Biotechnology, University of Verona, 37134 Verona, Italy*

Complete contact information is available at: https://pubs.acs.org/10.1021/acsfoodscitech.5c00022

Author Contributions

R.L.B. and N.F.L. contributed equally to this work.

Funding

The Ph.D. scholarship of N.F.L. was funded by REACT-EU FSE in the framework of PON "Ricerca e Innovazione" 2014−2020 (DM 1061/2021). Codice BIO13, DOT1340225, Borsa 1 CUP B39J21026610001.

Notes

The authors declare no competing financial interest.

ACKNOWLEDGMENTS

The authors thank Marta Purgato and Fabio Fracchetti for their technical assistance.

REFERENCES

(1) Alexandre, H.; Guilloux-Benatier, M. Yeast autolysis in sparkling wine - a review. *Aust. J. Grape Wine Res.* **2006**, *12*, 119−127.

(2) Vejarano, R. Non-*Saccharomyces* in winemaking: source of mannoproteins, nitrogen, enzymes, and antimicrobial compounds. *Fermentation* **2020**, *6*, 76.

(3) Schiavone, M.; Sieczkowski, N.; Castex, M.; Dague, E.; Marie François, J. Effects of the strain background and autolysis process on the composition and biophysical properties of the cell wall from two different industrial yeasts. *FEMS Yeast Res.* **2015**, *15* (2), 1−11.

(4) Gnoinski, G. B.; Schmidt, S. A.; Close, D. C.; Goemann, K.; Pinfold, T. L.; Kerslake, F. L. Novel methods to manipulate autolysis in sparkling wine: effects on yeast. *Molecules* **2021**, *26*, 387.

(5) Binati, R. L.; Ferremi Leali, N.; Avesani, M.; Salvetti, E.; Felis, G.; Monti, F.; Torriani, S. Application of FTIR microspectroscopy in oenology: shedding light on cell wall composition of *Saccharomyces cerevisiae* strains. *Food Bioprocess Technol.* **2023**, *17*, 1596−1609.

(6) Mihoubi, W.; Sahli, E.; Gargouri, A.; Amiel, C. FTIR spectroscopy of whole cells for the monitoring of yeast apoptosis mediated by p53 over-expression and its suppression by *Nigella sativa* extracts. *PLoS One* **2017**, *12*, e0180680.

(7) Vatanshenassan, M.; Boekhout, T.; Mauder, N.; Robert, V.; Maier, T.; Meis, J. F.; Berman, J.; Then, E.; Kostrzewa, M.; Hagen, F. Evaluation of microsatellite typing, ITS sequencing, AFLP fingerprinting, MALDI-TOF MS, and Fourier-transform infrared spectroscopy analysis of *Candida auris*. *J. Fungi* **2020**, *6* (3), 146.

(8) Dimopoulou, M.; Kefalloniti, V.; Tsakanikas, P.; Papanikolaou, S.; Nychas, G. E. Assessing the biofilm formation capacity of the wine spoilage yeast *Brettanomyces bruxellensis* through FTIR spectroscopy. *Microorganisms* **2021**, *9* (3), 587.

(9) Machová, E.; Fiačanová, L.; Čížová, A.; Korcová, J. Mannoproteins from yeast and hyphal form of *Candida albicans* considerably differ in mannan and protein content. *Carbohydr. Res.* **2015**, *408*, 12−17.

(10) Oelofse, A.; Malherbe, S.; Pretorius, I. S.; Du Toit, M. Preliminary evaluation of infrared spectroscopy for the differentiation of *Brettanomyces bruxellensis* strains isolated from red wines. *Int. J. Food Microbiol.* **2010**, *143*, 136−142.

(11) Grangeteau, C.; Gerhards, D.; Rousseaux, S.; von Wallbrunn, C.; Alexandre, H.; Guilloux-Benatier, M. Diversity of yeast strains of the genus *Hanseniaspora* in the winery environment: What is their involvement in grape must fermentation? *Food Microbiol* **2015**, *50*, 70−77.

(12) Grangeteau, C.; Gerhards, D.; Terrat, S.; Dequiedt, S.; Alexandre, H.; Guilloux-Benatier, M.; von Wallbrunn, C.; Rousseaux, S. FT-IR spectroscopy: A powerful tool for studying the inter- and intraspecific biodiversity of cultivable non-*Saccharomyces* yeasts isolated from grape must. *J. Microbiol. Methods* **2016**, *121*, 50−58.

(13) Moore, J. P.; Zhang, S. L.; Nieuwoudt, H.; Divol, B.; Trygg, J.; Bauer, F. F. A multivariate approach using attenuated total reflectance mid-infrared spectroscopy to measure the surface mannoproteins and β-glucans of yeast cell walls during wine fermentations. *J. Agric. Food Chem.* **2015**, *63*, 10054.

(14) Adt, I.; Kohler, A.; Gognies, S.; Budin, J.; Sandt, C.; Belarbi, A.; Manfait, M.; Sockalingum, G. D. FTIR spectroscopic discrimination of *Saccharomyces cerevisiae* and *Saccharomyces bayanus* strains. *Can. J. Microbiol.* **2010**, *56*, 793−801.

(15) Nguyen, T. D.; Guyot, S.; Pénicaud, C.; Passot, S.; Sandt, C.; Fonseca, F.; Saurel, R.; Husson, F. Understanding the responses of *Saccharomyces cerevisiae* yeast strain during dehydration processes using synchrotron infrared spectroscopy. *Analyst* **2017**, *142*, 3620−3628.

(16) Câmara Jr, A. A.; Nguyen, T. D.; Saurel, R.; Sandt, C.; Peltier, C.; Dujourdy, L.; Husson, F. Biophysical stress responses of the yeast *Lachancea thermotolerans* during dehydration using Synchrotron-FTIR Microspectroscopy. *Front. Microbiol.* **2020**, *11*, 11−14.

(17) Burattini, E.; Cavagna, M.; Dell'Anna, R.; Malvezzi Campeggi, F.; Monti, F.; Rossi, F.; Torriani, S. A FTIR microspectroscopy study of autolysis in cells of the wine yeast *Saccharomyces cerevisiae*. *Vib. Spectrosc.* **2008**, *47* (2), 139−147.

(18) Cavagna, M.; Dell'Anna, R.; Monti, F.; Rossi, F.; Torriani, S. Use of ATR-FTIR microspectroscopy to monitor autolysis of *Saccharomyces cerevisiae* cells in a base wine. *J. Agric. Food Chem.* **2010**, *58* (1), 39−45.

(19) Faustino, M.; Durão, J.; Pereira, C. F.; Oliveira, A. S.; Pereira, J. O.; Pereira, A. M.; Ferreira, C.; Pintado, M. E.; Carvalho, A. P. Comparative analysis of mannans extraction processes from spent yeast *Saccharomyces cerevisiae*. *Foods* **2022**, *11* (23), 3753.

(20) Malacrinò, P.; Zapparoli, G.; Tosi, E.; Dellaglio, F. Selection of indigenous *Saccharomyces* yeasts for production of Amarone wine. *Vignevini* **2005**, *32*, 131−135.

(21) Galichet, A.; Sockalingum, G. D.; Belarbi, A.; Manfait, M. FTIR spectroscopic analysis of *Saccharomyces cerevisiae* cell walls: study of

an anomalous strain exhibiting a pink-colored cell phenotype. *FEMS Microbiol. Lett.* **2001**, *197*, 179−186.
(22) R Core Team. *R: A Language and Environment for Statistical Computing*; R Foundation for Statistical Computing: 2023. www.R-project.org/.

https://doi.org/10.1021/acsfoodscitech.5c00022
ACS Food Sci. Technol. 2025, 5, 1625−1631